Published in final edited form as:
Mol Cell. 2015 February 19; 57(4): 648–661. doi:10.1016/j.molcel.2015.01.005.

Akt-mediated Phosphorylation of XLF Impairs Non-homologous End Joining DNA Repair

Pengda Liu[1,*], **Wenjian Gan**[1,*], **Chunguang Guo**[2], **Anyong Xie**[3,4], **Daming Gao**[1,5], **Jianping Guo**[1], **Jinfang Zhang**[1], **Nicholas Willis**[3], **Arthur Su**[2], **John M. Asara**[3], **Ralph Scully**[3], and **Wenyi Wei**[1,6]

[1]Department of Pathology, Beth Israel Deaconess Medical Center, Harvard Medical School, Boston, MA 02215, USA

[2]Howeard Hughes Medical Institute, the Children's Hospital, the Immune Disease Institute and Harvard Medical School, Boston, MA 02115, USA

[3]Department of Medicine, Beth Israel Deaconess Medical Center, Boston, MA 02215, USA

[4]Sir Run Run Shaw Hospital and Institute of Translational Medicine, Zhejiang University School of Medicine, Hangzhou, Zhejiang 310016, China

SUMMARY

Deficiency in repair of damaged DNA leads to genomic instability and is closely associated with tumorigenesis. Most DNA double-strand-breaks (DSBs) are repaired by two major mechanisms, homologous-recombination (HR) and non-homologous-end-joining (NHEJ). Although Akt has been reported to suppress HR, its role in NHEJ remains elusive. Here, we report that Akt phosphorylates XLF at Thr181 to trigger its dissociation from the DNA ligase IV/XRCC4 complex, and promotes its interaction with 14-3-3β leading to XLF cytoplasmic retention, where cytosolic XLF is subsequently degraded by $SCF^{\beta\text{-}TRCP}$ in a CKI-dependent manner. Physiologically, upon DNA damage, XLF-T181E expressing cells display impaired NHEJ and elevated cell death. Whereas a cancer-patient-derived XLF-R178Q mutant, deficient in XLF-T181 phosphorylation, exhibits an elevated tolerance of DNA damage. Together, our results reveal a pivotal role for Akt in suppressing NHEJ and highlight the tight connection between aberrant Akt

[6]To whom correspondence should be addressed: Wenyi Wei, Ph.D., Associate Professor, Department of Pathology, Beth Israel Deaconess Medical Center, Harvard Medical School, 3 Blackfan Circle, Boston, MA 02115, Phone: 617-735-2495; Fax: 617-735-2480, wwei2@bidmc.harvard.edu.
[5]Current address: Institute of Biochemistry and Cell Biology, Shanghai Institutes for Biological Sciences, Chinese Academy of Sciences, 320 Yue-yang Road, Shanghai 200031, China.
[*]These two authors contributed equally to this work.

Author Contributions

P.L., W.G. and W.W. designed experiments and wrote the manuscript. P.L. and W.G. performed most of the experiments with help from J.G., J. Z., N.W. and D.G. A.X. performed NHEJ assays in the mouse ES cells. C.G. and A.S. performed V(D)J recombination assays in B cells. W.W. and R.S. guided and supervised the project.

hyper-activation and deficiency in timely DSB repair, leading to genomic instability and tumorigenesis.

INTRODUCTION

DNA double-strand breaks (DSBs) are the most hazardous DNA lesions due to their ability to trigger chromosomal rearrangements if not repaired timely and efficiently, and have been considered a hallmark of tumorigenesis (Jackson, 2002; Khanna and Jackson, 2001). Therefore, multiple DSB sensing and DNA damage repair (DDR) mechanisms have evolved to govern genome stability (Ciccia and Elledge, 2010; Jackson and Durocher, 2013). The most well-studied DDR mechanism involves the cellular response to DSBs, initiated by activating the ATM (ataxia telangiectasia mutated) kinase to trigger phosphorylation of H2AX (pS139-H2AX) and MDC1 (mediator of DNA damage checkpoint protein 1), serving to recruit the E3 ligases RNF8 and RNF168 for a second wave of chromatin modifications largely by promoting K63-linkage polyubiquitination of histones (Huen et al., 2007; Kolas et al., 2007). These modifications subsequently recruit various DNA repair factors such as Rap80 (Sobhian et al., 2007) for repair of damaged DNA.

In eukaryotes, two mechanisms are primarily responsible for repairing DSBs: the non-homologous-end-joining (NHEJ) (Lieber, 2010) and the homologous recombination (HR) repair pathway (Dudas and Chovanec, 2004; Johnson and Jasin, 2001). HR, a highly accurate repair mechanism, requires similar or identical parental DNA strands as templates for repair. Therefore, it has been reported that HR repair is largely restrained in S/G2 cell phases when a second copy of the template DNA strand is present (Hartlerode et al., 2011; Karanam et al., 2012; Rothkamm et al., 2003). In addition, HR repair also occurs during DNA replication or gene transcription, as both cellular processes trigger endogenous DSBs in cells (Ghosal and Chen, 2013; Huang et al., 1998). Unlike HR, NHEJ does not require a repair template, instead this process involves the resection and digestion of the damaged DNA followed by direct ligation of processed DNA ends (Lieber et al., 2003). Hence, NHEJ is not restrained in a specific cell cycle phase (Mao et al., 2008). The imprecise nature of NHEJ is thought to facilitate accumulation of DNA mutations, which is critical for immune diversification in lymphocytes as well as for the selection of genetic changes favoring cancer or aging (Bunting and Nussenzweig, 2013).

Moreover, deficiency in repair of DSBs has also been observed closely associated with tumorigenesis (Helleday et al., 2008). Notably, elevated PI3K/Akt oncogenic signaling is considered as a hallmark of carcinomas (Fruman and Rommel, 2014; Testa and Tsichlis, 2005) and has been shown to promote genomic instability via various mechanisms. Specifically, elevated Akt activity leads to deficiencies in repairing damaged DNA by inactivating the G2 checkpoint (Xu et al., 2010), and phosphorylating Chk1 (checkpoint kinase 1) (Pedram et al., 2009), or through cytoplasmic retention of BRCA1 (breast cancer 1, early onset) (Plo et al., 2008; Tonic et al., 2010) or RPA (replication protein A) (Pedram et al., 2009) to block the resection process. However, the mechanistic role of Akt in NHEJ remains largely unknown (Xu et al., 2012). To this end, Akt has been reported to interact and regulate DNA-PK (DNA-dependent serine/threonine protein kinase) to facilitate the

recruitment of repair factors to DNA damage sites, while at later stages Akt triggered DNA-PK dissociation from the damage foci, indicating that Akt may play two opposing roles in regulating the loading and unloading of DNA-PK on DNA damage sites (Toulany et al., 2012). However, whether and how Akt may directly regulate NHEJ remains elusive.

Here we report that Akt phosphorylates XLF (XRCC4 like factor, also called NHEJ1) at T181, to dissociate XLF from the XRCC4 (X-ray repair cross-complementing protein 4)/DNA ligase IV (LIG4) complex and subsequently triggers XLF cytoplasmic translocation, leading to XLF ubiquitination by $SCF^{\beta\text{-}TRCP}$ in a CKI-dependent manner. Together, our findings reveal a signaling cascade in suppressing NHEJ through phosphorylation and degradation of XLF, and also provide a possible mechanistic explanation for the observed hyper-activation of Akt and deficiency in DNA damage repair in human cancers.

RESULTS

Hyper-activation of Akt leads to impaired DNA damage repair in cells

To examine the potential role of Akt in regulating NHEJ, we depleted endogenous PTEN (phosphatase and tensin homolog), a negative regulator of Akt activation (Stambolic et al., 1998) and observed that consistent with previous reports (Shen et al., 2007; Song et al., 2012), elevated Akt activity in PTEN-depleted cells (Figure 1A) led to increased basal DNA damage levels as evidenced by an increase in γ-H2AX staining (Figure 1B), delayed DNA repair responses post-IR (ionizing radiation) treatments (Figure 1B–C), as well as an increased cellular sensitivity to IR or bleocin challenges (Figure S1A–C). These results indicated that aberrant Akt activation may impair the DSB repair process. Consistent with this notion, ectopic expression of a cancer-derived oncogenic Akt mutant, E17K (Brugge et al., 2007), also led to a similarly reduced DSB repair efficiency post-IR treatments (Figure 1D–F). More importantly, in an experimental system with a single copy of both HR and NHEJ reporter (Weinstock et al., 2006) (Figure S1D–E), elevated Akt activation did not significantly affect HR (Figure 1G and Figure S1D), but led to reduced NHEJ repair efficiency (Figure 1H and Figure S1E), supporting that Akt might negatively regulate NHEJ.

Central to the NHEJ repair pathway is a protein complex containing LIG4, XRCC4 and XLF (Ahnesorg et al., 2006; Buck et al., 2006; Wilson et al., 1997) that form a filament-like structure (Hammel et al., 2010; Ropars et al., 2011) to bridge damaged DNA ends for efficient ligation (Andres et al., 2012). To pinpoint the primary target(s) for Akt kinase-activity-dependent suppression of NHEJ, we examined whether Akt could directly modify any of these three key NHEJ repair factors. To this end, we observed that only XLF, but not XRCC4 nor LIG4 exhibited Akt-dependent phosphorylation in cells (Figure 1I). As the MRN (Mre11-Rad51-Nbs1) complex has also been shown to play a critical role to recruit NHEJ repair factors to DNA damage sites (Quennet et al., 2011), we also examined whether any MRN components is potential Akt substrate(s). Notably, although human Mre11 was phosphorylated by Akt on T597 in cells (Figures S1F–G), its Akt consensus phosphorylation motif “RxRxxpS/pT” (Obata et al., 2000) is not conserved in other species (Figure S1H). Hence, in the remainder of studies, we focused on characterizing the possible role of Akt-mediated phosphorylation of XLF in governing NHEJ.

Akt1 phosphorylates XLF at the T181 residue *in vitro* and in cells

Consistent with Akt being a physiological kinase for XLF, inhibition of Akt by Akt inhibitor AktVIII or MK2206, or mTOR inhibitor pp242 significantly reduced XLF phosphorylation in cells. Furthermore, inhibition of Akt downstream kinases including mTORC1 (by rapamycin) or S6K1 (by S6K1-I) did not result in dramatically reduced XLF phosphorylation in cells (Figure 2A and Figure S2A). Interestingly, only Akt1, but not Akt2 or Akt3, nor other close AGC kinases including S6K1 or SGK1, triggered XLF phosphorylation in cells (Figure 2B–C). Moreover, insulin stimulation efficiently triggered the phosphorylation of endogenous XLF (Figure 2D). Importantly, upon DNA damage triggered by etoposide treatment, inhibition of DNA-PK by Nu7026 led to a reduction in XLF phosphorylation (Figure S2B). Furthermore, this effect could be largely rescued by expressing a constitutively-active Akt (Myr-Akt) or by insulin stimulation to trigger Akt activation independent of DNA-PK (Figure S2B), further supporting that Akt may be the major physiological kinase governing XLF phosphorylation in cells downstream of DNA-PK upon DNA damage (Bozulic et al., 2008).

Notably, we identified a putative Akt phosphorylation motif “RxRxxpS/pT” (Obata et al., 2000) located at T181 of XLF that is evolutionarily conserved (Figure 2E). Moreover, mutating T181 to an alanine diminished XLF phosphorylation induced by insulin (Figure 2F). Consistently, depletion of PTEN enhanced phosphorylation of WT-XLF, but not T181A-XLF (Figure 2G), indicating that in cells T181 is the primary Akt phosphorylation site, which is further confirmed by *in vitro* kinase assays (Figure 2H) and mass spectrometry analyses (Figure S2C).

Phosphorylation of XLF on T181 dissociates XLF from the LIG4/XRCC4 complex

We next examined whether Akt-mediated phosphorylation of XLF on T181 played any significant role in regulating NHEJ. To this end, we observed that XLF-T181 phosphorylation did not significantly affect the formation of XLF homo-dimers (Figure S3A), a process that has been revealed necessary for constructing LIG4/XRCC4/XLF filaments (Ropars et al., 2011). Moreover, as the integrity of the LIG4/XRCC4/XLF complex is required for efficient NHEJ activity (Ahnesorg et al., 2006), we continued to explore whether XLF phosphorylation may affect the association of XLF with LIG4 and/or XRCC4. Strikingly, the XLF phospho-mimetic mutant, T181E-XLF, largely lost its interaction with either XRCC4 or LIG4 both in cells (Figure 3A and Figure S3B–C) and *in vitro* (Figure 3B), suggesting that phosphorylation of XLF may negatively regulate the organization of the LIG4/XRCC4/XLF complex. Consistently, insulin-induced Akt activation led to phosphorylation of WT-, but not T181A- nor T181E-XLF, and subsequently resulted in XLF dissociation from the LIG4/XRCC4 complex (Figure 3C). Notably, the phospho-deficient T181A-XLF mutant exhibited a constitutive interaction with, while the phospho-mimetic T181E-XLF mutant was defective in association with LIG4 and XRCC4 regardless of insulin stimulation (Figure 3C). In addition, an inverse correlation between XLF phosphorylation and its binding to LIG4 and XRCC4 was observed post-IR treatments (Figure 3D).

As Akt-mediated phosphorylation of its substrates has been reported to trigger their cytoplasmic translocation in part via inducing binding 14-3-3 (Gao et al., 2009; Liang et al., 2002; Lin et al., 2009), we next examined whether XLF-T181 phosphorylation affected its sub-cellular localization. Notably, we identified a putative 14-3-3 binding motif evolutionarily conserved in XLF immediately adjacent to T181 (Figure 3E). WT-XLF, but not T181A-XLF, specifically interacted with 14-3-3β, but not other isoforms of 14-3-3 in cells (Figures 3F–G), supporting the notion that Akt-mediated XLF-T181 phosphorylation may trigger its association with 14-3-3β and subsequent cytoplasmic retention (Figure 3H). In echoing this finding, hyper-activation of Akt resulting from depletion of PTEN, led to increased cytoplasmic retention of endogenous XLF (Figure S3D). Additionally, mutation of P183 to an alanine, the critical residue in the canonical 14-3-3 binding motif, attenuated XLF interaction with 14-3-3β (Figure 3I), and retained not only WT-, but also T181E-XLF in the nucleus (Figure 3H), arguing for a critical role for XLF interaction with 14-3-3β for cytoplasmic retention of XLF. Interestingly, the P183A mutation also led to partially restored XLF interaction with both LIG4 and XRCC4 (Figure 3J), indicating that acquired interaction with 14-3-3β may play a critical role in blocking the interaction between XLF and the LIG4/XRCC4 complex in the nucleus. Notably, compared with WT-, T181E-XLF also displayed a significant deficiency in binding importin complexes that are responsible for transporting molecules into nucleus (Figure 3K–M), which might also in part contribute to the cytoplasmic retention of pT181-XLF.

Cytoplasmic pT181-XLF is targeted for $SCF^{\beta\text{-}TRCP}$-mediated ubiquitination and subsequent degradation in a CKI-dependent manner

Interestingly, cytoplasmic T181E-XLF was more unstable than its WT- counterpart (Figure 4A–B), suggesting that phosphorylation of XLF-T181 may negatively regulate XLF stability. As F-box proteins have been reported to regulate protein turnovers in a phosphorylation-dependent manner (Busino et al., 2003; Wang et al., 2014), we examined the association of XLF with a panel of F-box proteins. We found that XLF interacted with β-TRCP1 and Fbl18, and to a lesser extent, Fbl3a (Figure S4A). Furthermore, the presence of a putative β-TRCP-recognizable degron ($_{169}$ESGxT_{173}) in human XLF indicated a possible role for $SCF^{\beta\text{-}TRCP}$ in regulating XLF stability. In support of this notion, depletion of β-TRCP1 (Figure 4C–D and Figure S4B–C) or Cullin 1 (Figure 4E and Figure S4D–E) resulted in elevated abundance of endogenous XLF. More importantly, XLF interacted with Cullin 1 at endogenous levels (Figure S4F) and displayed a significantly reduced interaction with the R474A-β-TRCP1 mutant that is deficient in interacting with substrates (Gao et al., 2011) (Figure 4F).

Given that substrate phosphorylation is required for β-TRCP to target its substrate(s) for ubiquitination and subsequent degradation (Frescas and Pagano, 2008), assessing upstream kinases previously reported to be associated with $SCF^{\beta\text{-}TRCP}$-mediated proteolysis revealed that both CKIδ and CKIγ2 may participate in XLF degradation (Figure 4G). Importantly, CKI-mediated phosphorylation of WT-XLF, but not the degron-deficient XLF mutant (S170A/T173A, AA) (Figure 4H), triggered its association with β-TRCP1 *in vitro* (Figure S4G), further supporting CKI as a modifying enzyme to trigger XLF recognition by $SCF^{\beta\text{-}TRCP}$. In addition, T181E-, but not WT- nor T181A-XLF displayed an enhanced

ability to bind CKI in cells (Figure 4I), indicating that Akt-mediated XLF phosphorylation not only translocates XLF into the cytoplasm, but also may prime XLF for subsequent CKI phosphorylation. In echoing this notion, compared with WT-XLF, T181E-XLF displayed a stronger interaction with β-TRCP1 (Figure 4J). More importantly, physiological insulin stimulation led to a significantly shortened half-life of endogenous XLF (Figure S4H), which could in part be reversed by inhibiting CKI (Figure S4I), depleting endogenous β-TRCP1 or Cullin 1 (Figure S4I), or by reducing Akt activity through serum starvation (Figure S4J).

Consistent with S170/T173 being the major CKI phosphorylation sites to trigger XLF recognition and subsequent degradation by β-TRCP1, mutation of both residues to alanines largely diminished CKI-dependent phosphorylation of XLF *in vitro* (Figure S4K), and attenuated XLF interaction with β-TRCP1 in cells (Figure S4L). Furthermore, compared with WT-XLF, AA-XLF was deficient in ubiquitination triggered by $SCF^{\beta\text{-}TRCP}$ (Figure 4K), and resistant to CKI-induced XLF degradation (Figure 4L). Moreover, CKI-induced XLF degradation could be partially blocked by MG132 (Figure 4M), suggesting that XLF is largely degraded through the 26S proteasome. Notably, although Akt phosphorylated the phospho-degron-deficient XLF-AA mutant (Figure S4M), XLF-AA acquired resistance to β-TRCP-mediated degradation (Figure 4L), indicating that Akt phosphorylation of XLF-T181 only primes XLF for its subsequent phosphorylation and ubiquitination triggered by CKI, while CKI-mediated phosphorylation of XLF at the ESG degron (on S170 and T173) is the rate-limiting event governing XLF degradation (Figure S4N).

Akt-mediated XLF phosphorylation impairs NHEJ repair and V(D)J recombination

To further determine whether phosphorylation-mediated XLF dissociation from the LIG4/XRCC4 complex and cytoplasmic translocation is functionally important in cells, we examined whether Akt-dependent XLF-pT181 affects NHEJ repair in cells and *in vitro*. To this end, we utilized a patient-derived 2BN cell line, which lacks XLF expression (Ahnesorg et al., 2006), to generate derivative cell lines stably expressing WT- or T181E-XLF (Figure S5A). Compared with WT-XLF, T181E-XLF expressing 2BN cells exhibited delayed and deficient DNA repair (Figure 5A–B), suggesting that Akt-mediated XLF phosphorylation impairs the NHEJ process. Notably, T181E-XLF expressing cells displayed a reduced cellular survival rate post IR-treatments (Figure 5C). As Akt has been well characterized as a pro-survival factor, elevated Akt signaling may facilitate tumorigenesis by both impairing DNA repair and evading apoptosis (Toulany et al., 2012; Xu et al., 2012). As such, accumulation of unrepaired DSBs in the absence of pro-survival protection by Akt may lead to an elevated cell death in T181E-XLF expressing cells (Figure S5B).

Consistently, depletion of XLF significantly disrupted NHEJ, but not HR repair (Figure 5D and Figure S5C), which could be partially rescued by reintroducing WT-, but not T181E-XLF (Figure 5E and Figure S5D). In further support of the deleterious role of XLF-pT181 in NHEJ, LIG4/XRCC4/XLF complexes isolated from T181E-XLF expressing 2BN cells demonstrated a reduced DNA ligase activity *in vitro* compared to WT-XLF expressing cells (Figure 5F). Moreover, siRNA-mediated knockdown of XLF in mouse embryonic stem (ES) cells harboring a single copy of NHEJ reporter (Xie et al., 2007; Xie et al., 2009) led to a

significant reduction in NHEJ efficiency (Figure 5G), which could be partially rescued by re-expressing WT-, but not T181E-XLF (Figure 5G and Figure S5E). To further define a physiological role of XLF phosphorylation in regulating NHEJ and cell survival, we generated U2OS cell lines depleted of endogenous XLF (Figure S5F) and reconstituted with WT- or T181E-XLF (Figure S5G–I). Notably, depletion of endogenous XLF resulted in reduced colony formation post-IR treatments (Figure 5H). Importantly, this phenotype was partially rescued by re-introducing WT-, but not T181E-XLF (Figure 5H), emphasizing the negative role of XLF phosphorylation in NHEJ repair, which led to an accumulation of unrepaired DSBs to trigger cell death under DNA damage stress in the absence of Akt (Figure S5B). Consistently, depletion of PTEN led to sustained 53BP1 foci in cells expressing WT-XLF (Figure S5J, K and N), but not T181A-XLF (Figure 5I and Figure S5L–M).

In addition to NHEJ, the LIG4/XRCC4/XLF complex has also been shown to be indispensible for V(D)J recombination in B cells, and XLF is functionally redundant with ATM in this process (Zha et al., 2011). Notably, compared with WT-XLF, T181E-XLF led to attenuated V(D)J recombination in $XLF^{-/-}ATM^{\Delta/\Delta}$ pre-B cells (Figure S5O–P), further indicating a possible negative role of Akt-mediated XLF phosphorylation in regulating V(D)J recombination pathways. Similarly, B cell specific knockout of *Sin1*, the essential component of mTORC2 resulting in inactivation of Akt, has been reported to cause enhanced V(D)J recombination, supporting a critical role for Akt in negatively regulating V(D)J recombination (Lazorchak et al., 2010).

A patient-derived XLF-R178Q mutation displays an enhanced NHEJ repair ability through disrupting Akt-mediated XLF phosphorylation at T181

The observation that Akt-mediated phosphorylation of XLF compromised NHEJ suggests that human cancers may acquire elevated Akt activity to allow accumulation of genomic mutations in part via inactivating both NHEJ and cellular apoptosis pathways. In keeping with this notion, Akt has been reported to be tightly associated with resistance to chemo- and radio-therapies (Bussink et al., 2008; Kraus et al., 2002). However, as a counteracting mechanism, tumors may also develop chemo- or radio-therapeutic resistance in part by evading XLF-phosphorylation-mediated inactivation of NHEJ to acquire elevated capacity to repair DSBs during chemo- or radio-therapies. Interestingly, an XLF-R178Q mutation was identified in a colorectal cancer patient (TCGA case ID: TCGA-F5-6814). Importantly, this mutation disrupts the canonical Akt phosphorylation motif and prevents phosphorylation on T181 (Figures 6A–B). As a result, R178Q-XLF retains binding LIG4 and XRCC4 (Figure 6C), and displays cellular resistance to treatment with a chemotherapeutic drug, bleocin (Figure 6D). Importantly, similarly to T181A-XLF (Figure 5I), depletion of PTEN did not lead to sustained 53BP1 foci formation in R178Q-XLF expressing cells (Figure 6E–G), confirming that R178Q-XLF displays an enhanced NHEJ repair ability in cells. Together these results reveal that the cancer-derived XLF-R178Q mutation may confer cellular resistance to chemotherapeutic treatments in part by evading Akt-mediated XLF phosphorylation to retain NHEJ repair ability under excessive DNA damage stress, typically associated with chemo- or radio-therapies (Figure S6).

DISCUSSION

The NHEJ pathway serves as a major player in promoting genomic rearrangements (Gu et al., 2008). XLF, XRCC4 and LIG4 form a functional NHEJ complex, and mice with knockout of any individual component share common features of radio-sensitivity and defects in lymphocytes (Boboila et al., 2012; Chiang et al., 2012; Zhu et al., 2002). However, how this critical DSB repair complex is regulated *in vivo* to govern NHEJ remains largely unknown. To this end, our data reveals that Akt-mediated phosphorylation of XLF-T181 significantly impairs the NHEJ repair process, resulting in accumulation of unrepaired DSBs (Figure 7). Notably, the fluctuation of XLF phosphorylation inversely correlated with the integrity of LIG4/XRCC4/XLF complex post-IR treatment (Figure 3D), which peaked before and after the repair of damaged DNA. Our results thus suggest that upon DNA damage, inhibition of NHEJ by Akt-dependent phosphorylation of XLF might be released to allow repair of damaged DNA, followed by re-establishment of the inhibition by re-phosphorylation of XLF once the repair is complete (Figure 3D). However, additional in-depth studies are warranted to examine whether Akt-mediated phosphorylation of XLF may serve as a repair termination signal.

Furthermore, XLF phosphorylation was attenuated when Akt activation was largely suppressed by serum starvation for 36 hours (Figure S7A), resulting in an enhanced NHEJ efficiency compared with non-starved conditions (Figure S7B). Notably, 36-hour starvation only moderately affected HR (Figure S7C), in large due to its deficiency in arresting cell cycle in G0/G1 phases (Figure S7D). To further examine whether Akt-mediated XLF phosphorylation may serve as a general mechanism in suppressing NHEJ in proliferating cells, 72-hour serum starvation was employed. However, under this experimental condition, we found that DR-U2OS cells could not be fully arrested in G0/G1 in part due to the compromised $p14^{Arf}/p16^{INK4a}$ tumor suppressor pathways (Guan et al., 1994; Lukas et al., 1995; Stott et al., 1998). Notably, compared with cycling cells, XLF phosphorylation was reduced in 72-hour starved cells (Figure S7E). 72-hour serum starvation not only significantly attenuated HR (Figure S7F), but also led to an enhanced NHEJ repair ability in WT-XLF, but not T181A-XLF expressing cells (Figure S7G). These results indicate that elevated Akt activity in proliferating cells in large suppresses NHEJ through phosphorylating XLF-T181.

As a proto-oncogene, Akt has been well established to promote cell survival through blocking apoptosis (Franke et al., 2003). Thus it raises the question whether Akt could suppress NHEJ while promoting cell survival. To this end, we observed that under etoposide challenge, both XLF and several apoptosis-related Akt substrates were simultaneously phosphorylated by Akt (Figure S7I), suggesting that Akt could concurrently suppress NHEJ while protecting cells from apoptosis. More importantly, there is a marked decrease of pGSK3βpBad and pTSC2 in T181A-XLF expressing cells (Figure S7I), suggesting that the Akt phosphorylation-dependent cell survival protection mechanism may be in part deficient in cells with enhanced NHEJ ability via expressing T181A-XLF. These observations might be attributed to the extensive interplays between the Akt and DNA-PK signaling cascades. On one hand, DNA damage activates DNA-PK to trigger Akt activation (Bozulic et al., 2008). On the other hand, Akt could phosphorylate XLF to suppress NHEJ (Figure 7). In

this context, bypassing Akt-mediated suppression of NHEJ, such as in cells expressing T181A-XLF, may lead to more efficient repair of damaged DNA, therefore resulting in inactivation of DNA-PK and subsequently reduced Akt activity towards its downstream targets including GSK3β, Bad and TSC2 (Figure S7I). Consistently, upon DSBs triggered by bleocin treatment, PTEN depletion, which leads to Akt activation, protected T181E-XLF, but not T181A-XLF expressing cells from undergoing cell death (Figure S7J–K).

Moreover, we observed that under apoptotic stress without triggering DNA damage, such as Taxol or ABT-737 treatment, XLF phosphorylation appears not to play a significant role in regulating cellular survival (Figure S7L–M). These findings indicate that Akt-mediated XLF phosphorylation mainly affects cell fate under DNA damage conditions. Cumulatively, our results demonstrate that upon DNA damage, Akt could suppress NHEJ, potentially leading to accumulation of genetic mutations; meanwhile Akt could also provide anti-apoptotic protection to allow cells to select for favorable mutations, eventually facilitating tumorigenesis (Figure S7F). However, further investigation is required to understand the dynamic regulation of XLF by various upstream factors, as well as how deficiency in their crosstalk regulations may facilitate tumorigenesis.

EXPERIMENTAL PROCEDURES

Immunoblots and immunoprecipitation

Cells were lysed in EBC buffer (50 mM Tris pH 7.5, 120 mM NaCl, 0.5% NP-40) supplemented with protease inhibitors (Complete Mini, Roche) and phosphatase inhibitors (Calbiochem 524624 and 524625). The protein concentrations of lysates were measured by the Beckman Coulter DU-800 spectrophotometer using the Bio-Rad protein assay reagent. Same amounts of whole cell lysates were resolved by SDS-PAGE and immunoblotted with indicated antibodies. For immunoprecipitation, 1 mg lysates were incubated with the indicated antibody (1–2 μg) for 4 hr at 4 °C followed by 1 hr incubation with Protein A sepharose beads (GE Healthcare). Immunoprecipitates were washed five times with NETN buffer (20 mM Tris, pH 8.0, 100 mM NaCl, 1 mM EDTA and 0.5% NP-40) before being resolved by SDS-PAGE and immunoblotted with indicated antibodies.

In vivo homologous recombination assays

DR-U2OS cell lines with the integrated HR reporter DR-GFP and pCBASce-I expressing plasmid were kindly provided by Dr. Shiaw-Yih Lin from Memorial Sloan-Kettering Cancer Center (New York, NY). Assays were performed as described previously (Nakanishi et al., 2005; Peng et al., 2009). Briefly, cells were transfected with pCBASce-I and 48 hr later were subjected to flow cytometry analysis to quantify GFP positive cells. Cells were incubated in sodium butyrate (5 mM) for 16 hr to induce chromatin relaxation before analysis by flow cytometry.

In vivo Non-homologous end joining (NHEJ) repair assays

NHEJ repair analysis was performed as described previously (Nakanishi et al., 2005; Peng et al., 2009). Briefly, genomic DNA was isolated from mock- or I-SceI-transfected cells. PCR

was performed using primers DRGFP-F: CTGCTAACCATGTTCATGCC and DRGFP-R: AAGTCGTGCTGCTTCATGTG. PCR products were digested with I-SceI or I-SceI+BcgI.

In vitro ligation assays

In vitro DNA ligation assays were performed according to the protocol as described (O'Driscoll et al., 2001) with minor modifications.

Clonogenic survival assays

Cells were seeded in 6-well plates (800 cells/well) for 24 hr and irradiated with dose as indicated or treated with bleocin for 24 hr. Bleocin containing medium was then removed and replaced with fresh media. Cells were left for 8–12 days until formation of visible colonies. Colonies were washed with PBS and fixed with 10% acetic acid/10% methanol for 20 min, then stained with 0.4% crystal violet/20% ethanol for 20 min. After staining, the plates were washed with distilled water and air-dried.

Supplementary Material

Refer to Web version on PubMed Central for supplementary material.

Acknowledgments

We thank Brian North, Alan Lau, Hiroyuki Inuzuka and other members of the Wei laboratory for critical reading of the manuscript, Catherin Yan for providing valuable reagents, Min Yuan and Susanne Breitkopf for mass spectrometry experiments and members of the Wei and Scully laboratories for useful discussions. W.W. is an ACS scholar. P.L. is supported by 1K99CA181342. This work was supported in part by the NIH grants (R01CA177910 and R01GM094777 to W.W.; R01GM073894 and R01CA095175 to R.S.).

References

Ahnesorg P, Smith P, Jackson SP. XLF interacts with the XRCC4-DNA ligase IV complex to promote DNA nonhomologous end-joining. Cell. 2006; 124:301–313. [PubMed: 16439205]

Andres SN, Vergnes A, Ristic D, Wyman C, Modesti M, Junop M. A human XRCC4-XLF complex bridges DNA. Nucleic Acids Res. 2012; 40:1868–1878. [PubMed: 22287571]

Boboila C, Oksenych V, Gostissa M, Wang JH, Zha S, Zhang Y, Chai H, Lee CS, Jankovic M, Saez LM, et al. Robust chromosomal DNA repair via alternative end-joining in the absence of X-ray repair cross-complementing protein 1 (XRCC1). Proc Natl Acad Sci U S A. 2012; 109:2473–2478. [PubMed: 22308491]

Bozulic L, Surucu B, Hynx D, Hemmings BA. PKBalpha/Akt1 acts downstream of DNA-PK in the DNA double-strand break response and promotes survival. Mol Cell. 2008; 30:203–213. [PubMed: 18439899]

Brugge J, Hung MC, Mills GB. A new mutational AKTivation in the PI3K pathway. Cancer Cell. 2007; 12:104–107. [PubMed: 17692802]

Buck D, Malivert L, de Chasseval R, Barraud A, Fondaneche MC, Sanal O, Plebani A, Stephan JL, Hufnagel M, le Deist F, et al. Cernunnos, a novel nonhomologous end-joining factor, is mutated in human immunodeficiency with microcephaly. Cell. 2006; 124:287–299. [PubMed: 16439204]

Bunting SF, Nussenzweig A. End-joining, translocations and cancer. Nature reviews Cancer. 2013; 13:443–454.

Businо L, Donzelli M, Chiesa M, Guardavaccaro D, Ganoth D, Dorrello NV, Hershko A, Pagano M, Draetta GF. Degradation of Cdc25A by beta-TrCP during S phase and in response to DNA damage. Nature. 2003; 426:87–91. [PubMed: 14603323]

Bussink J, van der Kogel AJ, Kaanders JH. Activation of the PI3-K/AKT pathway and implications for radioresistance mechanisms in head and neck cancer. Lancet Oncol. 2008; 9:288–296. [PubMed: 18308254]

Chiang C, Jacobsen JC, Ernst C, Hanscom C, Heilbut A, Blumenthal I, Mills RE, Kirby A, Lindgren AM, Rudiger SR, et al. Complex reorganization and predominant non-homologous repair following chromosomal breakage in karyotypically balanced germline rearrangements and transgenic integration. Nat Genet. 2012; 44:390–397. S391. [PubMed: 22388000]

Ciccia A, Elledge SJ. The DNA damage response: making it safe to play with knives. Mol Cell. 2010; 40:179–204. [PubMed: 20965415]

Dudas A, Chovanec M. DNA double-strand break repair by homologous recombination. Mutat Res. 2004; 566:131–167. [PubMed: 15164978]

Franke TF, Hornik CP, Segev L, Shostak GA, Sugimoto C. PI3K/Akt and apoptosis: size matters. Oncogene. 2003; 22:8983–8998. [PubMed: 14663477]

Frescas D, Pagano M. Deregulated proteolysis by the F-box proteins SKP2 and beta-TrCP: tipping the scales of cancer. Nature reviews Cancer. 2008; 8:438–449.

Fruman DA, Rommel C. PI3K and cancer: lessons, challenges and opportunities. Nat Rev Drug Discov. 2014; 13:140–156. [PubMed: 24481312]

Gao D, Inuzuka H, Tan MK, Fukushima H, Locasale JW, Liu P, Wan L, Zhai B, Chin YR, Shaik S, et al. mTOR drives its own activation via SCF(betaTrCP)-dependent degradation of the mTOR inhibitor DEPTOR. Mol Cell. 2011; 44:290–303. [PubMed: 22017875]

Gao D, Inuzuka H, Tseng A, Chin RY, Toker A, Wei W. Phosphorylation by Akt1 promotes cytoplasmic localization of Skp2 and impairs APCCdh1-mediated Skp2 destruction. Nat Cell Biol. 2009; 11:397–408. [PubMed: 19270695]

Ghosal G, Chen J. DNA damage tolerance: a double-edged sword guarding the genome. Translational cancer research. 2013; 2:107–129. [PubMed: 24058901]

Gu W, Zhang F, Lupski JR. Mechanisms for human genomic rearrangements. Pathogenetics. 2008; 1:4. [PubMed: 19014668]

Guan KL, Jenkins CW, Li Y, Nichols MA, Wu X, O'Keefe CL, Matera AG, Xiong Y. Growth suppression by p18, a p16INK4/MTS1- and p14INK4B/MTS2-related CDK6 inhibitor, correlates with wild-type pRb function. Genes Dev. 1994; 8:2939–2952. [PubMed: 8001816]

Hammel M, Yu Y, Fang S, Lees-Miller SP, Tainer JA. XLF regulates filament architecture of the XRCC4.ligase IV complex. Structure. 2010; 18:1431–1442. [PubMed: 21070942]

Hartlerode A, Odate S, Shim I, Brown J, Scully R. Cell cycle-dependent induction of homologous recombination by a tightly regulated I-SceI fusion protein. PLoS One. 2011; 6:e16501. [PubMed: 21408059]

Helleday T, Petermann E, Lundin C, Hodgson B, Sharma RA. DNA repair pathways as targets for cancer therapy. Nature reviews Cancer. 2008; 8:193–204.

Huang M, Zhou Z, Elledge SJ. The DNA replication and damage checkpoint pathways induce transcription by inhibition of the Crt1 repressor. Cell. 1998; 94:595–605. [PubMed: 9741624]

Huen MS, Grant R, Manke I, Minn K, Yu X, Yaffe MB, Chen J. RNF8 transduces the DNA-damage signal via histone ubiquitylation and checkpoint protein assembly. Cell. 2007; 131:901–914. [PubMed: 18001825]

Jackson SP. Sensing and repairing DNA double-strand breaks. Carcinogenesis. 2002; 23:687–696. [PubMed: 12016139]

Jackson SP, Durocher D. Regulation of DNA damage responses by ubiquitin and SUMO. Mol Cell. 2013; 49:795–807. [PubMed: 23416108]

Johnson RD, Jasin M. Double-strand-break-induced homologous recombination in mammalian cells. Biochem Soc Trans. 2001; 29:196–201. [PubMed: 11356153]

Karanam K, Kafri R, Loewer A, Lahav G. Quantitative live cell imaging reveals a gradual shift between DNA repair mechanisms and a maximal use of HR in mid S phase. Mol Cell. 2012; 47:320–329. [PubMed: 22841003]

Khanna KK, Jackson SP. DNA double-strand breaks: signaling, repair and the cancer connection. Nat Genet. 2001; 27:247–254. [PubMed: 11242102]

Kolas NK, Chapman JR, Nakada S, Ylanko J, Chahwan R, Sweeney FD, Panier S, Mendez M, Wildenhain J, Thomson TM, et al. Orchestration of the DNA-damage response by the RNF8 ubiquitin ligase. Science. 2007; 318:1637–1640. [PubMed: 18006705]

Kraus AC, Ferber I, Bachmann SO, Specht H, Wimmel A, Gross MW, Schlegel J, Suske G, Schuermann M. In vitro chemo- and radio-resistance in small cell lung cancer correlates with cell adhesion and constitutive activation of AKT and MAP kinase pathways. Oncogene. 2002; 21:8683–8695. [PubMed: 12483521]

Lazorchak AS, Liu D, Facchinetti V, Di Lorenzo A, Sessa WC, Schatz DG, Su B. Sin1-mTORC2 suppresses rag and il7r gene expression through Akt2 in B cells. Mol Cell. 2010; 39:433–443. [PubMed: 20705244]

Liang J, Zubovitz J, Petrocelli T, Kotchetkov R, Connor MK, Han K, Lee JH, Ciarallo S, Catzavelos C, Beniston R, et al. PKB/Akt phosphorylates p27, impairs nuclear import of p27 and opposes p27-mediated G1 arrest. Nat Med. 2002; 8:1153–1160. [PubMed: 12244302]

Lieber MR. The mechanism of double-strand DNA break repair by the nonhomologous DNA end-joining pathway. Annu Rev Biochem. 2010; 79:181–211. [PubMed: 20192759]

Lieber MR, Ma Y, Pannicke U, Schwarz K. Mechanism and regulation of human non-homologous DNA end-joining. Nat Rev Mol Cell Biol. 2003; 4:712–720. [PubMed: 14506474]

Lin HK, Wang G, Chen Z, Teruya-Feldstein J, Liu Y, Chan CH, Yang WL, Erdjument-Bromage H, Nakayama KI, Nimer S, et al. Phosphorylation-dependent regulation of cytosolic localization and oncogenic function of Skp2 by Akt/PKB. Nat Cell Biol. 2009; 11:420–432. [PubMed: 19270694]

Lukas J, Parry D, Aagaard L, Mann DJ, Bartkova J, Strauss M, Peters G, Bartek J. Retinoblastoma-protein-dependent cell-cycle inhibition by the tumour suppressor p16. Nature. 1995; 375:503–506. [PubMed: 7777060]

Mao Z, Bozzella M, Seluanov A, Gorbunova V. DNA repair by nonhomologous end joining and homologous recombination during cell cycle in human cells. Cell Cycle. 2008; 7:2902–2906. [PubMed: 18769152]

Nakanishi K, Yang YG, Pierce AJ, Taniguchi T, Digweed M, D'Andrea AD, Wang ZQ, Jasin M. Human Fanconi anemia monoubiquitination pathway promotes homologous DNA repair. Proc Natl Acad Sci U S A. 2005; 102:1110–1115. [PubMed: 15650050]

O'Driscoll M, Cerosaletti KM, Girard PM, Dai Y, Stumm M, Kysela B, Hirsch B, Gennery A, Palmer SE, Seidel J, et al. DNA ligase IV mutations identified in patients exhibiting developmental delay and immunodeficiency. Mol Cell. 2001; 8:1175–1185. [PubMed: 11779494]

Obata T, Yaffe MB, Leparc GG, Piro ET, Maegawa H, Kashiwagi A, Kikkawa R, Cantley LC. Peptide and protein library screening defines optimal substrate motifs for AKT/PKB. J Biol Chem. 2000; 275:36108–36115. [PubMed: 10945990]

Pedram A, Razandi M, Evinger AJ, Lee E, Levin ER. Estrogen inhibits ATR signaling to cell cycle checkpoints and DNA repair. Mol Biol Cell. 2009; 20:3374–3389. [PubMed: 19477925]

Peng G, Yim EK, Dai H, Jackson AP, Burgt I, Pan MR, Hu R, Li K, Lin SY. BRIT1/MCPH1 links chromatin remodelling to DNA damage response. Nat Cell Biol. 2009; 11:865–872. [PubMed: 19525936]

Plo I, Laulier C, Gauthier L, Lebrun F, Calvo F, Lopez BS. AKT1 inhibits homologous recombination by inducing cytoplasmic retention of BRCA1 and RAD51. Cancer Res. 2008; 68:9404–9412. [PubMed: 19010915]

Quennet V, Beucher A, Barton O, Takeda S, Lobrich M. CtIP and MRN promote non-homologous end-joining of etoposide-induced DNA double-strand breaks in G1. Nucleic Acids Res. 2011; 39:2144–2152. [PubMed: 21087997]

Ropars V, Drevet P, Legrand P, Baconnais S, Amram J, Faure G, Marquez JA, Pietrement O, Guerois R, Callebaut I, et al. Structural characterization of filaments formed by human Xrcc4-Cernunnos/XLF complex involved in nonhomologous DNA end-joining. Proc Natl Acad Sci U S A. 2011; 108:12663–12668. [PubMed: 21768349]

Rothkamm K, Kruger I, Thompson LH, Lobrich M. Pathways of DNA double-strand break repair during the mammalian cell cycle. Mol Cell Biol. 2003; 23:5706–5715. [PubMed: 12897142]

Shen WH, Balajee AS, Wang J, Wu H, Eng C, Pandolfi PP, Yin Y. Essential role for nuclear PTEN in maintaining chromosomal integrity. Cell. 2007; 128:157–170. [PubMed: 17218262]

Sobhian B, Shao G, Lilli DR, Culhane AC, Moreau LA, Xia B, Livingston DM, Greenberg RA. RAP80 targets BRCA1 to specific ubiquitin structures at DNA damage sites. Science. 2007; 316:1198–1202. [PubMed: 17525341]

Song MS, Salmena L, Pandolfi PP. The functions and regulation of the PTEN tumour suppressor. Nat Rev Mol Cell Biol. 2012; 13:283–296. [PubMed: 22473468]

Stambolic V, Suzuki A, de la Pompa JL, Brothers GM, Mirtsos C, Sasaki T, Ruland J, Penninger JM, Siderovski DP, Mak TW. Negative regulation of PKB/Akt-dependent cell survival by the tumor suppressor PTEN. Cell. 1998; 95:29–39. [PubMed: 9778245]

Stott FJ, Bates S, James MC, McConnell BB, Starborg M, Brookes S, Palmero I, Ryan K, Hara E, Vousden KH, et al. The alternative product from the human CDKN2A locus, p14(ARF), participates in a regulatory feedback loop with p53 and MDM2. EMBO J. 1998; 17:5001–5014. [PubMed: 9724636]

Testa JR, Tsichlis PN. AKT signaling in normal and malignant cells. Oncogene. 2005; 24:7391–7393. [PubMed: 16288285]

Tonic I, Yu WN, Park Y, Chen CC, Hay N. Akt activation emulates Chk1 inhibition and Bcl2 overexpression and abrogates G2 cell cycle checkpoint by inhibiting BRCA1 foci. J Biol Chem. 2010; 285:23790–23798. [PubMed: 20495005]

Toulany M, Lee KJ, Fattah KR, Lin YF, Fehrenbacher B, Schaller M, Chen BP, Chen DJ, Rodemann HP. Akt promotes post-irradiation survival of human tumor cells through initiation, progression, and termination of DNA-PKcs-dependent DNA double-strand break repair. Mol Cancer Res. 2012; 10:945–957. [PubMed: 22596249]

Wang Z, Liu P, Inuzuka H, Wei W. Roles of F-box proteins in cancer. Nature reviews Cancer. 2014; 14:233–247.

Weinstock DM, Nakanishi K, Helgadottir HR, Jasin M. Assaying double-strand break repair pathway choice in mammalian cells using a targeted endonuclease or the RAG recombinase. Methods in enzymology. 2006; 409:524–540. [PubMed: 16793422]

Wilson TE, Grawunder U, Lieber MR. Yeast DNA ligase IV mediates non-homologous DNA end joining. Nature. 1997; 388:495–498. [PubMed: 9242411]

Xie A, Hartlerode A, Stucki M, Odate S, Puget N, Kwok A, Nagaraju G, Yan C, Alt FW, Chen J, et al. Distinct roles of chromatin-associated proteins MDC1 and 53BP1 in mammalian double-strand break repair. Mol Cell. 2007; 28:1045–1057. [PubMed: 18158901]

Xie A, Kwok A, Scully R. Role of mammalian Mre11 in classical and alternative nonhomologous end joining. Nat Struct Mol Biol. 2009; 16:814–818. [PubMed: 19633669]

Xu N, Hegarat N, Black EJ, Scott MT, Hochegger H, Gillespie DA. Akt/PKB suppresses DNA damage processing and checkpoint activation in late G2. J Cell Biol. 2010; 190:297–305. [PubMed: 20679434]

Xu N, Lao Y, Zhang Y, Gillespie DA. Akt: a double-edged sword in cell proliferation and genome stability. J Oncol. 2012; 2012:951724. [PubMed: 22481935]

Zha S, Guo C, Boboila C, Oksenych V, Cheng HL, Zhang Y, Wesemann DR, Yuen G, Patel H, Goff PH, et al. ATM damage response and XLF repair factor are functionally redundant in joining DNA breaks. Nature. 2011; 469:250–254. [PubMed: 21160472]

Zhu C, Mills KD, Ferguson DO, Lee C, Manis J, Fleming J, Gao Y, Morton CC, Alt FW. Unrepaired DNA breaks in p53-deficient cells lead to oncogenic gene amplification subsequent to translocations. Cell. 2002; 109:811–821. [PubMed: 12110179]

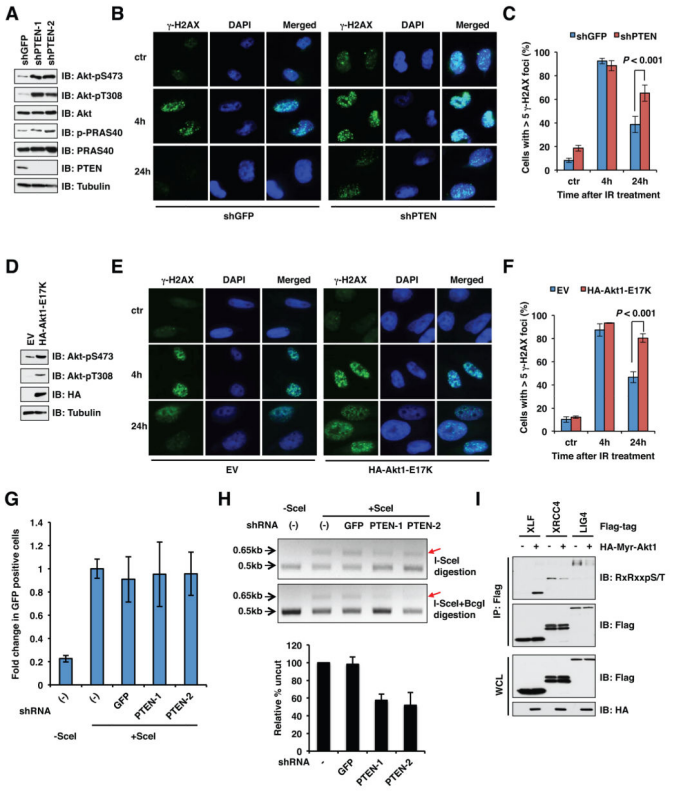

Figure 1. Hyperactivation of Akt leads to impaired DNA damage repair in cells

A. Depletion of PTEN led to elevated Akt activation. Immunoblot (IB) of whole cell lysates (WCLs) derived from U2OS cells depleted of PTEN by two independent shRNAs (shGFP as a negative control).

B. Representative immuno-fluorescent images of γ-H2AX foci in either shGFP or shPTEN U2OS cells generated in (**A**) upon IR treatment (10 Gy) for the indicated time periods.

C. Quantification of γ-H2AX positive cells in (**B**). n≥100 cells from each sample were counted. Data were shown as mean ± s.d. for three independent experiments. $p<0.001$ was calculated by Student's *t* test.

D. Expression of Akt1-E17K led to elevated Akt activation. IB of WCLs derived from U2OS cells stably expressing HA-Akt1-E17K via viral infection.

E–F. Representative immuno-fluorescent images of γ-H2AX staining (**E**) and quantification (**F**) of γ-H2AX positive cells in indicated U2OS cells generated in (**D**) upon IR treatment (10Gy) for the indicated time periods. Data were shown as mean ± s.d. for three independent experiments. $p<0.001$ was calculated by Student's *t* test.

G. PTEN depletion did not significantly affect HR. Quantitative summary of the percentages of GFP+ cells in I-SceI-transfected U2OS cells depleted of indicated molecules. Data were shown as mean ± s.d. for three independent experiments.

H. PTEN depletion attenuated NHEJ. Representative images of PCR products digested by I-*Sce*I or I-*Sce*I + *Bcg*I. Please refer to the methods section for experimental details.

I. XLF, but not XRCC4 nor LIG4 was phosphorylated by Akt in cells. IB of WCLs and Flag-immunoprecipitates (IP) derived from HeLa cells transfected with indicated plasmids. (see also Figure S1)

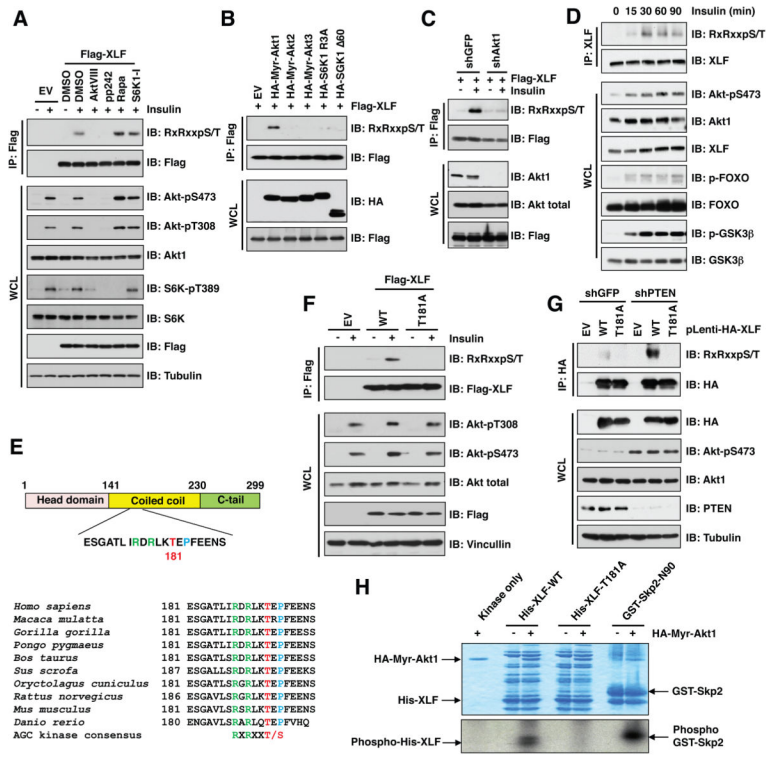

Figure 2. Akt1 phosphorylates XLF at T181

A. Immunoblot (IB) analysis of whole-cell lysates (WCL) and anti-Flag immunoprecipitates (IP) derived from Flag-XLF-transfected HeLa cells that were serum-starved for 24 hr and then collected after 100 nM insulin stimulation for 30 min. Where indicated, the kinase inhibitors (AktVIII, 10 μM; PP242, 1 μM; rapamycin, 20 nM; S6K1-I, 10 μM) were added together with insulin.

B. Akt1 phosphorylated XLF in cells. IB analysis of WCLs and Flag-IPs derived from HEK293T cells transfected with indicated constructs.

C. IB analysis of WCLs and Flag-IPs derived from HeLa cells depleted of endogenous Akt1 (shGFP as a negative control) transfected with Flag-XLF. Where indicated, cells were serum starved for 24 hr and stimulated by insulin (100 nM) for 30 min before collection.

D. IB analysis of WCLs and endogenous XLF-IPs derived from HEK293 cells. Where indicated, cells were serum starved for 24 hr and stimulated by insulin (100 nM) for the indicated periods before harvesting.

E. A schematic presentation of the evolutionarily conserved Thr 181 residue in XLF.

F. XLF was phosphorylated on T181. IB analysis of WCLs and Flag-IPs derived from HeLa cells transfected with indicated Flag-XLF and serum starved for 24 hr before stimulation by insulin (100 nM) for 30 min.

G. IB analysis of WCLs and HA-IPs derived from U2OS cells depleted of PTEN (shGFP as a negative control) stably expressing WT- or T181A-XLF by lenti-viral infections.

H. *In vitro* kinase assays depicting major Akt phosphorylation sites in XLF.

(see also Figure S2)

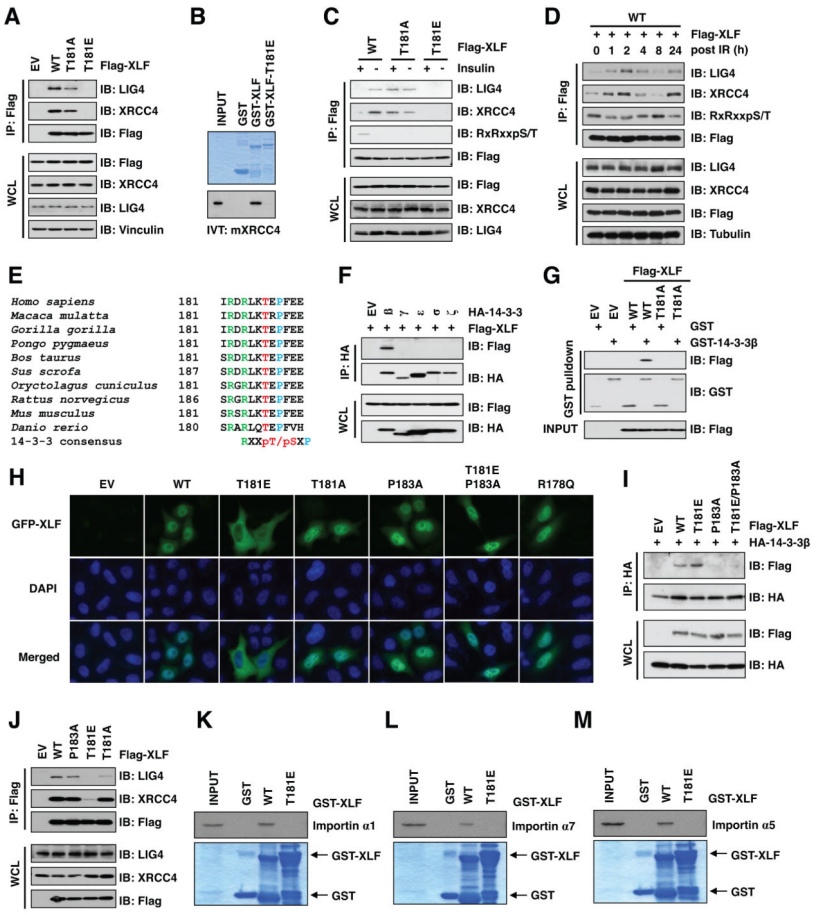

Figure 3. XLF phosphorylation on T181 dissociates XLF from the DNA ligase IV/XRCC4 complex, triggers its binding with 14-3-3 to translocate XLF into the cytoplasm

A. Immunoblot (IB) analysis of whole-cell lysates (WCL) and anti-Flag immunoprecipitates (IP) derived from HEK293T cells transfected with the indicated constructs.

B. GST pull down assays to demonstrate that T181E-XLF abolished its interaction with *in vitro* translated (IVT) XRCC4.

C. IB analysis of WCLs and Flag-IPs derived from HeLa cells transfected with indicated constructs serum-starved for 24 hr and stimulated by insulin (100 nM) for 30 min.

D. IB analysis of WCLs and Flag-IPs derived from Flag-XLF-transfected HeLa cells treated with 10 Gy irradiation and collected after the indicated time periods.

E. A schematic presentation of the evolutionarily conserved putative 14-3-3 binding site P183 within XLF.

F. XLF specifically interacted with 14-3-3β. IB analysis of WCLs and HA-IPs derived from HeLa cells transfected with Flag-XLF and indicated HA-14-3-3 constructs.

G. T181A-XLF lost binding with 14-3-3β. GST-14-3-3β fusion proteins were used as a bait to pull down either WT or T181A-XLF expressed in HEK293T cells.

H. Representative GFP fluorescence images. XLF was tagged with EGFP. Nuclei were stained with DAPI.

I. IB analysis of WCLs and HA-IPs derived from HEK293T cells transfected with indicated Flag-XLF constructs with HA-14-3-3β.

J. IB analysis of WCLs and Flag-IPs derived from HEK293T cells transfected with indicated constructs.

K–M. T181E-XLF was deficient in binding importin complexes. Importin components α1 (**K**), α5 (**L**) and α7 (**M**) were translated *in vitro* and used in GST-XLF pull down assays. (see also Figure S3)

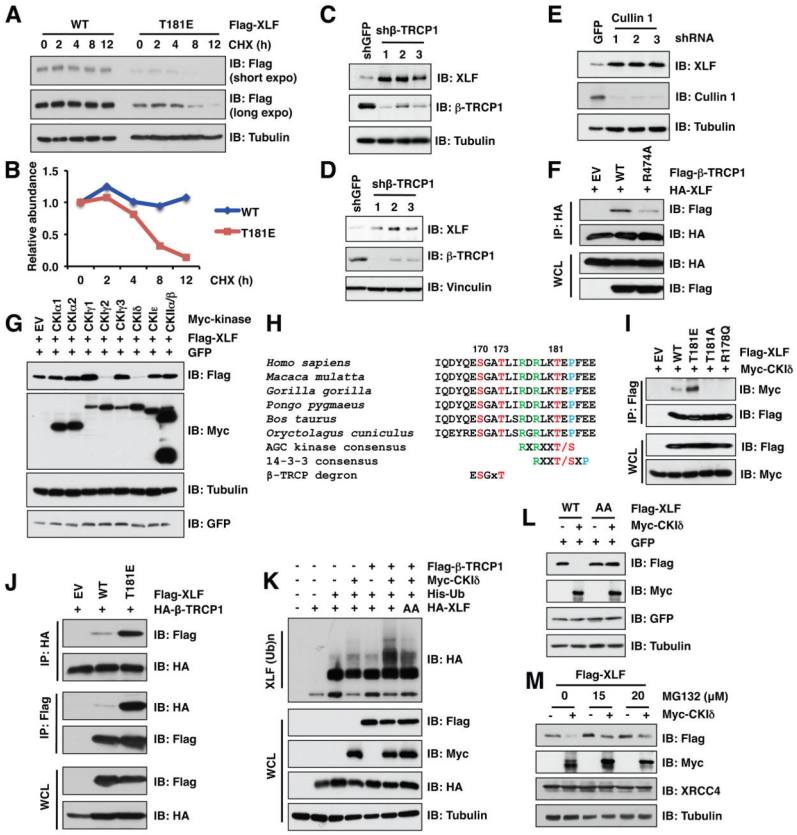

Figure 4. Cytoplasmic pT181-XLF is targeted for β-TRCP-mediated ubiquitination and degradation in a CKI-dependent manner

A. T181E-XLF displayed a significantly shortened half-life than WT-XLF in cells. Immunoblot (IB) analysis of whole cell lysates (WCL) derived from HeLa cells transfected with indicated Flag-XLF. 36 hr post transfection, 100 μM cycloheximide (CHX) was added and cells were harvested at indicated time points.

B. XLF protein abundance in (**A**) was quantified by ImageJ and plotted as indicated.

C–D. Depletion of endogenous β-TRCP1 led to upregulated XLF expression in cells. IB analysis of WCLs derived from HEK293 (**C**) or DR-U2OS (**D**) cells depleted of endogenous β-TRCP1 by three independent shRNAs (shGFP as a negative control).

E. Depletion of Cullin 1 led to upregulated XLF expression in cells. IB analysis of WCLs derived from PC3 cells depleted of endogenous Cullin 1 by three independent shRNAs (shGFP as a negative control).

F. Substrate-binding deficient β-TRCP1 (R474A) displayed reduced interaction with XLF in cells. IB analysis of WCLs and HA-IPs derived from HEK293T cells transfected with HA-XLF and indicated Flag-β-TRCP1 constructs.

G. Specific CKI isoforms promoted XLF degradation in cells. IB analysis of WCLs derived from HEK293T cells transfected with Flag-XLF, GFP and indicated Myc-CKI or CKII constructs.

H. Sequence alignment to reveal that both S170 and T173 sites are conserved through evolution.

I. CKIδ preferred T181E-XLF to WT-XLF for interaction. IB analysis of WCLs and Flag-IPs derived from HEK293T cells transfected with indicated constructs. 12 hr before harvesting, 20 μM MG132 was added.

J. β-TRCP1 preferred T181E-XLF to WT-XLF for interaction. IB analysis of WCLs and Flag- or HA-IPs derived from HEK293T cells transfected with indicated constructs. 12 hr before harvesting, 20 μM MG132 was added.

K–L. XLF-S170A/T173A (AA) was deficient in ubiquitination (**K**) and CKI-mediated degradation (**L**) in cells. IB analysis of WCLs (**K, L**) and His pull-downs (**K**) derived from HEK293T cells transfected with indicated constructs.

M. IB analysis of WCLs and His pull-downs derived from HEK293T cells transfected with indicated constructs. Where indicated, MG132 was added for 12 hr before harvest.

(see also Figure S4)

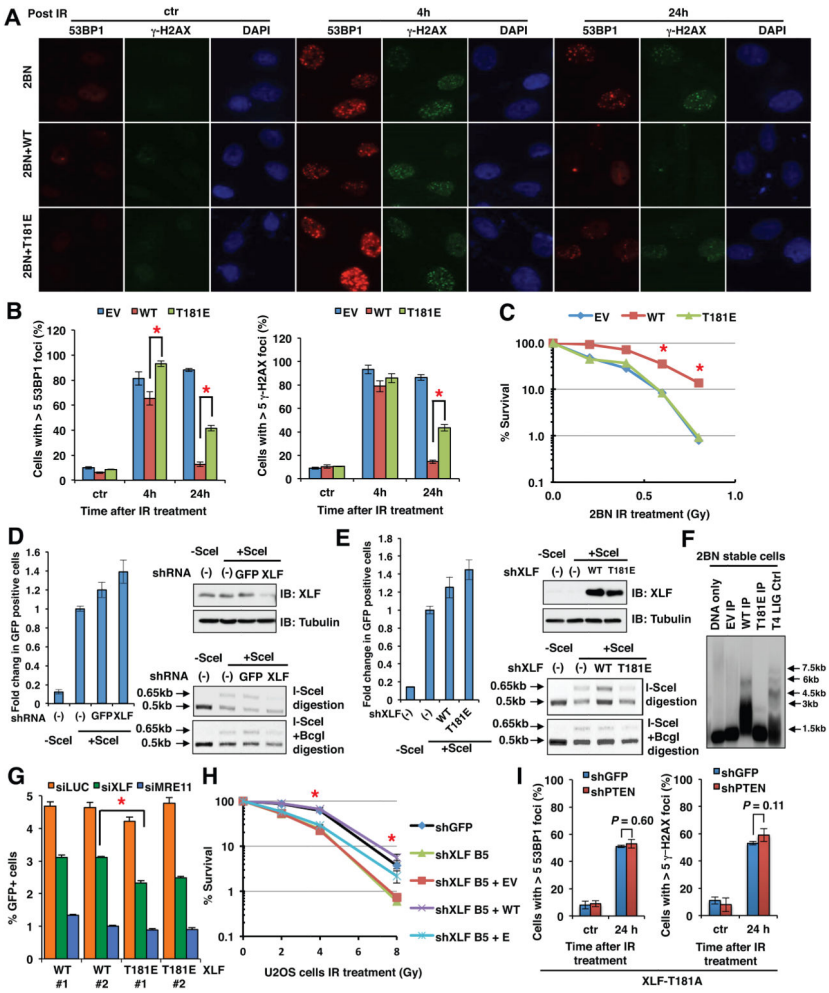

Figure 5. Akt-mediated XLF phosphorylation impairs NHEJ and V(D)J recombination

A. Representative immune-fluorescent images of 53BP1 and γ-H2AX staining in indicated 2BN cells generated in (**A**) upon IR treatment (3 Gy) for the indicated time periods.

B. Compared with WT-XLF, T181E-XLF expressing 2BN cells retained more 53BP1 foci and γ-H2AX foci post-IR treatment (3 Gy). Quantification of 53BP1 foci and γ-H2AX foci formation at the indicated time period post IR treatment; results are shown as means ± s.d. for three independent experiments. At least 100 cells were scored in each sample for each experiment. * indicates $p<0.05$ by Student's *t* test.

C. 1,000 2BN cells stably expressing WT- or T181E-XLF were treated with γ-irradiation of indicated doses and seeded on P100 dishes. 30 days later the numbers of formed colonies were counted. The graphs show the mean ± s.d. for three independent experiments. * indicates $p<0.05$ by Student's *t* test.

D–E. XLF depletion (**D**) or expressing T181E-XLF (**E**) significantly affected NHEJ, but not HR to repair DSBs induced by I-*Sce* I in DR-U2OS cells. Left, quantitative summary of the percentages of GFP+ cells in I-SceI-transfected cells, which were shown as mean ± s.d. for three independent experiments. Right, representative images of PCR products digested by I-*Sce*I or I-*Sce*I + *Bcg*I. * indicates $p<0.05$ by Student's *t* test.

F. T181E-XLF containing complexes were deficient in ligating DNA *in vitro*. HA-immunoprecipitates derived from 2BN cells stably expressing HA-WT- or HA-T181E-XLF were used as the ligase to ligate random blunt-ended 1.5 kb DNA dsDNA fragments generated by PCR *in vitro*.

G. T181E-XLF displayed deficiency in rescuing NHEJ in mouse ES cells. T181E- or WT-XLF was introduced into mouse ES cells harboring a single copy of NHEJ reporter, followed by depletion of endogenous, but not exogenous expressed XLF. NHEJ efficiency of resulting cells were measured by FACS. The graphs show mean ± s.d. for three independent experiments. * indicates $p<0.05$ by Student's *t* test

H. T181E-XLF could not rescue DNA damage stress-induced cell death. WT- or T181E-XLF stably expressing U2OS cells depleted of endogenous XLF were treated by the indicated doses of IR. 8–12 days post-treatment, survived colonies were counted. The graphs show the mean ± s.d. for three independent experiments. * indicates $p<0.05$ by student's *t* test.

I. PTEN depletion didn't significantly affect 53BP1 and γ-H2AX foci formation post-IR treatment in XLF-T181A expressing U2OS cells. Quantification of 53BP1 and γ-H2AX foci at the indicated time period post IR treatment (10 Gy). Results are shown as means ± s.d for three independent experiments. n≥100 cells were scored in each sample for each experiment. (see also Figure S5)

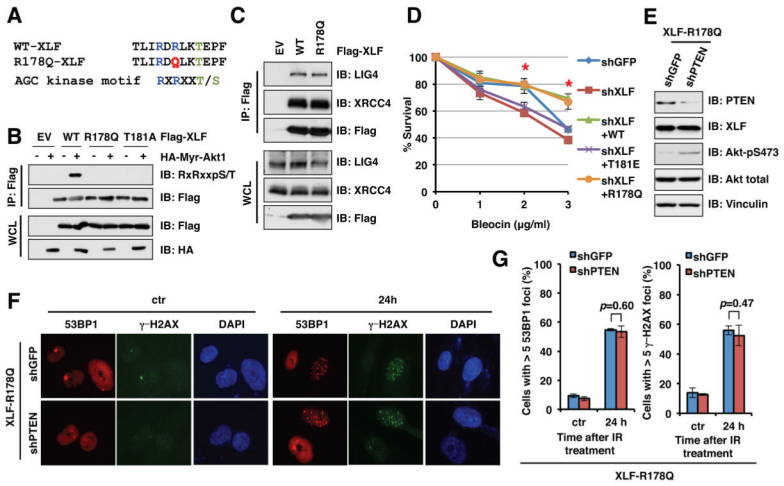

Figure 6. A patient-derived XLF-R178Q mutation displays enhanced NHEJ repair ability through disrupting Akt-mediated XLF phosphorylation at T181

A. Illustration of how XLF-R178Q disrupted the canonical Akt phosphorylation motif.

B. XLF-R178Q abolished Akt-mediated XLF-T181 phosphorylation. Immunoblot (IB) analysis of whole cell lysates (WCL) and Flag-immunoprecipitates (IP) derived from HEK293T cells transfected with indicated constructs.

C. XLF-R178Q retained interaction with LIG4 and XRCC4 in cells. IB analysis of WCLs and Flag-IPs derived from HEK293T cells transfected with indicated Flag-XLF constructs.

D. R178Q-XLF effectively rescued DNA damage-induced cell death. U2OS cells stably expressing WT-, T181E- or R178Q-XLF (with endogenous XLF depleted) were treated with indicated doses of bleocin for 24 hr before changing to normal media. 8–12 days post-treatment, survived colonies were counted and plotted. The graphs show mean ± s.d. for three independent experiments. * indicates $p<0.05$ by Student's *t* test.

E. IB of WCLs derived from U2OS cells depleted of PTEN (shGFP as a negative control).

F. Representative immuno-fluorescent images of 53BP1 and γ-H2AX foci in cells generated in (**E**) upon IR treatment (10 Gy) for the indicated time periods.

G. Depletion of PTEN didn't significantly affect 53BP1 and γ-H2AX foci formation post-IR treatment in XLF-R178Q expressing U2OS cells. Quantification of 53BP1 and γ-H2AX foci at the indicated time period post-IR treatment (10 Gy) from three independent experiments; results are shown as means ± s.d. At least 100 cells were scored in each sample for each experiment.

(see also Figure S6)

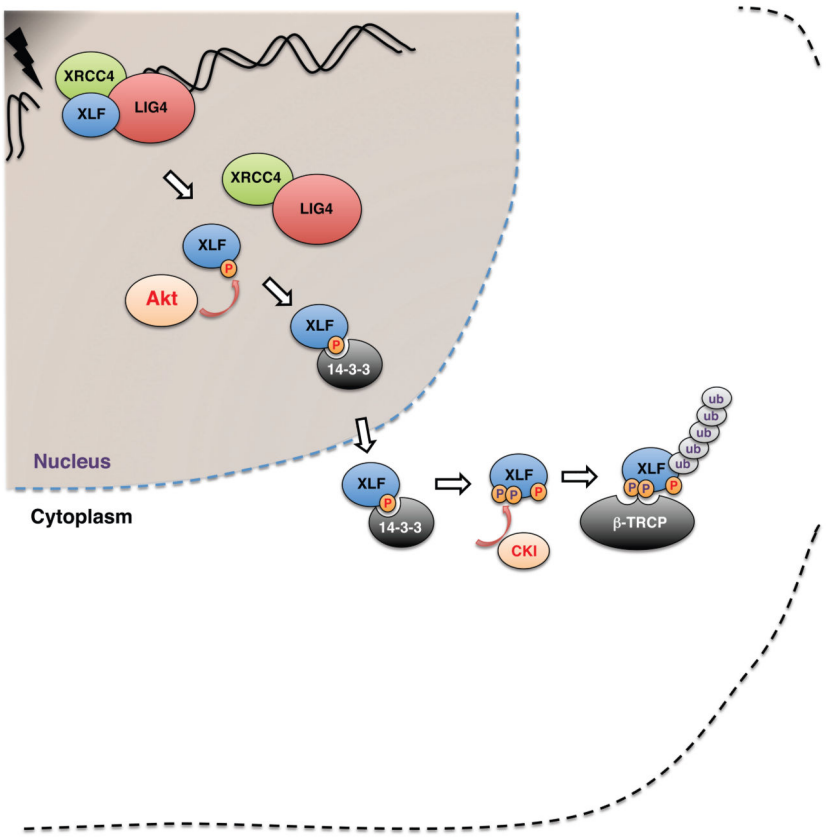

Figure 7. A proposed model illustrating how Akt-mediated phosphorylation of XLF leads to impaired NHEJ, XLF cytoplasmic translocation and subsequent degradation

XLF complexes with LIG4 and XRCC4 to form a NHEJ complex to repair DSBs. Akt-mediated phosphorylation of XLF-T181 dissociates XLF from NHEJ repair complex and triggers 14-3-3 binding to translocate XLF to cytoplasm, where cytosolic XLF could be further phosphorylated by CKI on S170 and T173 to trigger its recognition by β-TRCP for subsequent ubiquitination and degradation, thus terminating the NHEJ pathway.
(see also Figure S7)